Preparation, Evaluation, and *In Vitro* Release Study of *O*-Carboxymethyl Chitosan Nanoparticles Loaded with Gentamicin and Salicylic Acid

Jingou Ji, Shilei Hao, Jin Dong, Danjun Wu, Bin Yang, Yi Xu

Faculty of Pharmacy, College of Chemistry and Chemical Engineering, University of Chongqing, Chongqing 400030, China

Received 21 July 2010; accepted 4 April 2011
DOI 10.1002/app.34631
Published online 19 August 2011 in Wiley Online Library (wileyonlinelibrary.com).

ABSTRACT: To inhibit the ototoxicity of gentamicin (GM) and overcome the drawback related to chitosan (CS) nanoparticles preparation in acid solution, *O*-carboxymethyl chitosan (*O*-CMC) nanoparticles loaded with GM and salicylic acid (SA) were prepared by ionic cross-linking method using calcium chloride as crosslinking agent. The Fourier transform infrared (FTIR) spectroscopy and X-ray diffraction (XRD) were used to analyze the reaction of *O*-CMC and crosslinking agent. The parameters of preparation of the compound nanoparticles including the concentration of *O*-CMC, the mass ratio of *O*-CMC to calcium chloride, and the feed ratio of SA to GM were investigated. The results showed that the obtained nanoparticles had a high zeta potential and drug-loading capacity. The nanoparticles were characterized by a spherical morphology, with average size ranging from 148 to 345 nm and a narrow particle size distribution. *In vitro* release studies in phosphate buffer saline (pH 7.4) evidenced a burst release in the first 1 h, followed by a sustained release in the residual time. The release amount of SA and GM were approximately equal in 24 h, which indicated that the SA- and GM-loaded *O*-CMC nanoparticles are a promising carrier system for inhibiting the ototoxicity of GM. © 2011 Wiley Periodicals, Inc. J Appl Polym Sci 123: 1684–1689, 2012

Key words: carboxymethyl chitosan; gentamicin; ototoxicity; salicylic acid

INTRODUCTION

Gentamicin (GM), a complex of aminoglycoside antibiotic, is an abroad-spectrum antibiotic produced by various species of micromonospora under aerobic conditions.[1] The serious limitations of GM are the nephrotoxic and ototoxic side effects in therapeutic application. The ototoxicity of GM is based on the complex compound formed by GM with iron, which is capable of catalyzing the formation of free radicals *in vitro* and *in vivo*.[2,3] Therefore, a large number of free radical scavengers and iron chelators, such as deferoxamine, aminoguanidine, and salicylic acid (SA), have been used to attenuate the ototoxicity of GM successfully.[4–7] And, acetyl salicylate (aspirin) can significantly attenuate the risk of GM-induced hearing loss in clinical trial.[8] However, the separate injection of the GM (once a day) and SA (twice a day) makes the treatment inconvenient for the patient. Furthermore, reactive oxygen species generated in the recipient's cells will immediately react with the vicinal macromolecules, due to their high activity.[9] To inhibit the ototoxicity of GM effectively, the scavengers should react with the free radicals at fast speed when they are produced. But the separated injection may result in poor coordination between GM and SA in terms of the absorption and distribution *in vivo*, thus reducing the antagonism effect of SA.

Over the past few decades, nanoparticles have been used as various water soluble/insoluble medicine carriers for the controlled and site-specific delivery of drugs.[10] Nanoparticles have a lot of advantages such as protecting the drug from degradation prematurely, improving the intracellular penetration and retention time.[11,12] To date, different kinds of polymers such as chitosan (CS), polylactic acid (PLA), and poly(glycolide) acid have been used for the preparation of nanoparticles. Among them, CS has been intensively used in many areas including drug delivery system and tissue engineering due to its good biological properties in terms of good biocompatibility, biodegradability, and nontoxicity.[13,14] However, the poor water solubility of CS (only soluble in weak acidic solution) is one of the main drawbacks for its application in drug delivery

Correspondence to: J. Ji (jingou_ji@yahoo.com.cn).
Contract grant sponsor: Chongqing University Postgraduates' Science and Innovation Fund; contract grant number: 201005A1A0010333.
Contract grant sponsor: 211 Project Innovation Personnel Training Plan Items of Chongqing University; contract grant number: S-09103.

system.[15,16] *O*-Carboxymethyl chitosan (*O*-CMC) is a water soluble CS derivative, which has many outstanding properties including nontoxicity, biodegradability, biocompatibility, antibacterial activity, and improvement of the retention time and antifungal bioactivity.[17,18] Furthermore, the *O*-CMC nanoparticles could be synthesized via the crosslinking method between carboxyl (COOH) of *O*-CMC and calcium ion in neutral or weakly basic pH range, without the need of any acidic solution.

In this article, *O*-CMC nanoparticles loading with GM and SA have been prepared and used to inhibit the ototoxicity of GM. The physicochemical properties of *O*-CMC nanoparticles were tested by transmission electron microscopy (TEM), scanning electron microscope (SEM), X-ray diffraction (XRD), and Fourier transform infrared (FTIR) spectroscopy. The releasing properties of the drug-loaded nanoparticles in phosphate buffer saline (PBS) were also examined.

EXPERIMENTAL

Materials

O-CMC (Deacetylation degree 90%, introduced 90% *O*-carboxymethyl groups per repeating unit) was purchased from Qingdao Honghai Bio-tech (Shandong, China). GM was purchased from North China Pharmaceutical (Hebei, China). SA was purchased from Hezhong Bio-Chemical (Wuhan, China). Calcium chloride was purchased from Chuandong Chemical (Chongqing, China). All other materials and reagents used in the study were analytical grade.

Preparation of compound *O*-CMC nanoparticles

O-CMC nanoparticles were prepared via the crosslinking method between *O*-CMC and calcium chloride as described in literature.[19] Different concentrations (from 0.1 to 0.5%, w/v) of *O*-CMC solution were prepared by dissolving *O*-CMC in distilled water, the pH of *O*-CMC was adjusted 7.2, followed by flush mixing the solution with GM (0.2%, w/v) and SA (0.1%, w/v) solution, the total mass of drugs were 4 mg. The *O*-CMC nanoparticles formed spontaneously when the calcium chloride (0.4%, w/v) solution was added to the mixture by dropwise. The selected mass ratio of *O*-CMC to calcium chloride was from 2.5 to 5.0. The nanoparticle suspensions were continuously stirred for 1 h and centrifuged at 16,000 rpm for 30 min. The resulting nanoparticle products were lyophilized and stored.

Characterization of the nanoparticles

Particle size and zeta potential studies

Particle size, zeta potential, and polydispersity index (PDI) of nanoparticles were measured by dynamic light scattering using Nano ZS90 Zetasizer (Malvern Instruments, United Kingdom). Samples were diluted to appropriate concentrations with deionized water.

Surface morphology studies

The surface morphology of nanoparticles was examined by TEM and SEM. For TEM, the nanoparticles solution was dropped on copper grids and natively stained by 2% phosphotungstic acid. Sample was dried at room temperature and then examined by Tecrai 10 TEM (Philips, Dutch). For SEM, the nanoparticles suspensions were spread on a glass plate and dried at room temperature. The dried nanoparticles were gold sputtered and observed using an S-3400N microscope (Hitachi, Japan).

Fourier transform infrared spectral studies

The chemical structure and complexes formation of *O*-CMC, GM, SA, and *O*-CMC compound nanoparticles were analyzed by FTIR (Nicolet, USA). Samples for FTIR were prepared by grinding the dry specimens with KBr and pressing them to form disks.

X-ray diffraction studies

The XRD experiments were carried out on both the drug-loaded nanoparticles and pristine drugs using XRD 6000X diffract meter (Shimadzu, Japan).

Evaluation of drug loading capacity

The encapsulation efficiency (EE) and loading capacity (LC) of nanoparticles were determined as follow: 20 mg of drug-loaded nanoparticles was taken into 5 mL 0.1 mol/L HCl for 24 h. The nanoparticles suspension was separated by centrifugation at 16, 000 g for 30 min. The contents of GM and SA in the supernatant were analyzed by UV spectrophotometer at 248 nm and 297 nm. A blank sample was made from nanoparticles without loaded drugs but treated similarly as the drugs-loaded nanoparticles. All samples were measured in triplicate. The EE and LC were calculated by the following equations:

$$EE_{1,2} = \frac{F_{1,2}}{T_{1,2}} \times 100\%$$

$$LC_{1,2} = \frac{F_{1,2}}{W} \times 100\%$$

$F_{1,2}$ are the free GM and SA in the supernatant, $T_{1,2}$ are the feed amount of GM and SA, W is the total weight of lyophilized nanoparticles.

TABLE I
Characteristics of the GM/SA-Loaded *O*-CMC Nanoparticles for Different *O*-CMC Concentration (mean ± SD, $n = 3$)

O-CMC concentration (%)	SA		GM		Size		Zeta potential (mV)
	EE (%)	LC (%)	EE (%)	LC (%)	nm	PDI	
0.1	92.07 ± 3.10	36.34 ± 2.14	92.03 ± 1.51	23.90 ± 1.84	159.8 ± 10.2	0.111 ± 0.002	−35.64 ± 1.27
0.2	92.24 ± 3.01	36.89 ± 1.74	92.72 ± 2.07	24.72 ± 2.10	211.3 ± 15.9	0.012 ± 0.007	−34.07 ± 3.21
0.3	91.99 ± 2.01	35.84 ± 1.46	90.44 ± 2.37	23.49 ± 2.84	256.8 ± 10.9	0.079 ± 0.008	−33.67 ± 1.29
0.4	91.77 ± 1.20	35.30 ± 1.97	90.02 ± 3.18	23.08 ± 2.31	270.6 ± 8.2	0.128 ± 0.011	−32.95 ± 0.87
0.5	91.69 ± 3.16	31.26 ± 1.27	89.83 ± 2.83	20.42 ± 2.19	318.7 ± 9.1	0.094 ± 0.007	−32.17 ± 1.28

In vitro drug release studies

GM/SA loaded *O*-CMC nanoparticles and 5 mL PBS (pH 7.4) were put into dialysis bag (MWCO: 12,000). The dialysis bag was placed into 50 mL PBS and shaken at 100 stocks/min at 37°C. At specific time intervals, 5 mL release medium was collected and replaced with fresh PBS (5 mL). The concentrations of the released GM and SA in release medium were determined by UV spectrophotometer. The analysis was performed in triplicate for each sample.

RESULTS AND DISCUSSION

Preparation of *O*-CMC nanoparticles containing GM and SA

The *O*-CMC nanoparticles were prepared by ionic crosslinking method. The effects of different concentration of *O*-CMC (from 0.1 to 0.5%) on the characteristics of nanoparticles are shown in Table I. There were slight trends of EE, LC of SA, and GM by varying the concentration of *O*-CMC, the nanoparticles had exhibited higher EE and LC for both SA and GM when the *O*-CMC concentration was 0.2%, while lowest values were obtained for concentrations of 0.5%. This can be explained by considering that the high *O*-CMC concentration would result in highly viscous of the gelatin medium and hinder the encapsulation of drug into the *O*-CMC nanoparticles, and low *O*-CMC concentrations would also reduce the extent of crosslinking, which constitutes an obstacle to encapsulation. The residual carboxylate ions ($-COO^-$) would be responsible for the negative zeta potential, which can greatly influence the stability of the colloidal suspension. The increase of *O*-CMC concentration led to a decrease of zeta potential (in absolute value), which could explain that SA is contribute to the negative zeta potential under the weak base solution, and the LC of SA decrease with the increase of concentration of *O*-CMC.

The effect of the *O*-CMC/calcium chloride mass ratios in the range between 2.5 and 5.0 was also investigated. The EE, LC, particle size, and zeta potential of the nanoparticles are shown in Table II. Nanoparticle size, LC, and EE were all found to slightly increase with reducing the *O*-CMC/calcium chloride mass ratio. On the other side, the zeta potential decreased (in absolute value) for increasing amounts of calcium chloride. This surface charge loss could be related to the higher quenching activity at increased Ca^{2+} concentrations.

SA and GM loaded *O*-CMC nanoparticles having constant total drug amount and different SA to GM feed ratios ranging from 1.0 to 2.5 were also studied; the results are shown in Table III. The LC of GM became smaller and opposite trend was found for SA, as the feed ratio of SA to GM increased, which was consistent with the previous report.[20] The particle size and zeta potential were slightly affected by the increase feeding ratio.

Characterization of the GM/SA-loaded *O*-CMC nanoparticles

Figure 1(A,B) shows the surface morphology of the drugs loaded *O*-CMC nanoparticles. The TEM analysis shows that the *O*-CMC nanoparticles had spherical morphology, and the average diameter was

TABLE II
Effect of *O*-CMC/Calcium Chloride Mass Ratio on Characteristics of the GM/SA-Loaded *O*-CMC Nanoparticles (mean ± SD, $n = 3$)

O-CMC/calcium chloride mass ratio	SA		GM		Size		Zeta potential (mV)
	EE (%)	LC (%)	EE (%)	LC (%)	nm	PDI	
2.5	92.80 ± 2.30	44.90 ± 1.54	98.02 ± 1.28	31.62 ± 3.11	234.4 ± 10.3	0.138 ± 0.008	−28.92 ± 0.39
3.0	92.75 ± 1.26	44.88 ± 2.10	94.39 ± 2.37	30.45 ± 2.14	230.0 ± 9.7	0.038 ± 0.009	−30.43 ± 1.57
3.5	92.68 ± 0.38	40.89 ± 1.58	93.79 ± 2.41	27.58 ± 1.87	221.5 ± 11.0	0.118 ± 0.012	−32.42 ± 3.24
4.0	92.65 ± 1.98	38.08 ± 1.26	92.08 ± 1.92	25.23 ± 1.39	215.8 ± 16.3	0.133 ± 0.006	−33.04 ± 1.69
4.5	92.26 ± 3.01	36.90 ± 1.74	91.67 ± 2.07	24.45 ± 2.10	211.3 ± 15.9	0.012 ± 0.007	−34.07 ± 3.21
5.0	92.14 ± 2.11	34.99 ± 0.24	91.47 ± 1.34	23.16 ± 1.63	201.4 ± 20.3	0.020 ± 0.011	−34.31 ± 2.51

TABLE III
Effect of Different Feed Ratio of SA to GM on Characteristics of the GM/SA-Loaded *O*-CMC Nanoparticles (mean ± SD, $n = 3$)

Feed ratio (SA to GM)	SA		GM		Size		Zeta potential (mV)
	EE (%)	LC (%)	EE (%)	LC (%)	Nm	PDI	
1.0	91.70 ± 2.11	35.94 ± 2.14	83.14 ± 1.57	26.28 ± 3.12	228.6 ± 12.7	0.082 ± 0.005	−35.79 ± 4.10
1.5	92.26 ± 3.01	36.90 ± 1.74	91.67 ± 2.07	24.45 ± 2.10	215.8 ± 15.9	0.012 ± 0.007	−34.07 ± 3.21
2.0	94.12 ± 1.24	37.64 ± 1.84	100.00 ± 2.11	17.40 ± 1.49	200.4 ± 19.9	0.061 ± 0.010	−34.50 ± 1.98
2.5	91.94 ± 1.31	38.31 ± 1.92	100.00 ± 2.54	12.38 ± 1.71	218.5 ± 20.4	0.088 ± 0.006	−35.66 ± 2.14

about 200 nm [Fig. 1(A)]. Figure 1(B) shows the SEM analysis of the drug-loaded *O*-CMC nanoparticles, the nanoparticles also had spherical morphology, and the particles size was about 200 nm, which were similar with the TEM observed.

Figure 2 depicts the FTIR spectra of the unloaded *O*-CMC, the drug loaded *O*-CMC nanoparticles, GM and SA. Figure 2(A) shows the basic characteristic of *O*-CMC at 3431cm^{-1} could be attributed to the stretching vibration of the —NH_2 and —OH groups. The peaks at 2926 cm^{-1} and the strong peak at 1600 cm^{-1} correspond to the aliphatic C—H bond stretching and the N—H bending, respectively. The one at 1408 cm^{-1} could be assigned to the respective asymmetry and symmetry stretching vibration of COO—, and the peak at 1325 cm^{-1} can be attributed to the C—O stretching. Finally, another strong peak at 1074 cm^{-1} corresponds to the secondary hydroxyl group C—O, which indicates that the carboxymethyl substitution occurs at the C_6 position.[21] Figure 2(B) shows the characteristic peaks of GM including at 3250 cm^{-1} correspond to the —NH_2 bond stretching and the —OH groups stretching vibration and at 1610 cm^{-1} can be attributed to the N—H group bending.

As a consequence of the drug incorporation nanoparticles [Fig. 2(C)] a series of changes in the FTIR spectra were observed with respect to the unloaded *O*-CMC [Fig. 2(A)]: a shift of the peak associated to the stretching vibration of —NH_2 group and —OH group to a lower wavenumber (3412 cm^{-1}), a significant shift of the peak at 2926 cm^{-1}, assigned to C—H stretching vibration, to higher wavenumber (2949 cm^{-1}), and a weakening of the peak at 1325 cm^{-1}, which indicated that the crosslinking reaction between carboxyl groups of *O*-CMC and Ca^{2+} ions had occurred. Furthermore, the new peak at 1761 cm^{-1} indicates the reaction of —NH_2 group of GM and the —COOH group of *O*-CMC has occurred. And, the characteristic absorption peaks of SA [Fig. 2(D)] at 1700 and 1650 cm^{-1} corresponding to acetoxy group and carboxylic group bending shifts to 1580 cm^{-1}, respectively, which are due to the interaction between carboxylic —COOH group of SA and primary amide of CS.[22,23] These indicate that SA and GM have been loaded successfully into the *O*-CMC nanoparticles.

The X-ray diffractograms of SA, GM, drug unloaded, and drug loaded *O*-CMC nanoparticles are shown in Figure 3. As visible, SA pattern was characterized by four strong peaks at 2θ angles of 11°, 17°, 25°, and 32.5° [Fig. 3(A)], whereas GM pattern consisted of a broad shoulder at 20° [Fig. 3(B)]. Unloaded *O*-CMC exhibited one characteristic peak at 2θ of 20° [Fig. 3(C)], which became even broader in the diffraction pattern of drug-loaded *O*-CMC nanoparticles the peak at 20° [Fig. 3(D)], accompanied by the absence of characteristic peaks of SA and GM. It is well known that the width of XRD peak is related to the size of crystallite, the broadened peak usually resulting from small crystallites. The observed peak broadening for the drug-loaded *O*-CMC may be due the crosslinking reaction

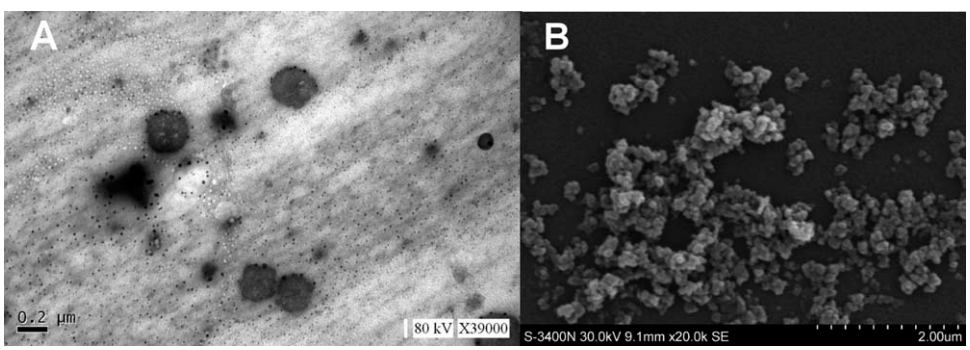

Figure 1 (A) TEM and (B) SEM photograph of the SA/GM-loaded *O*-CMC nanoparticles (*O*-CMC concentration 0.2%, *O*-CMC/calcium chloride mass ratio 4.5, Feed ratio of SA to GM 1.5).

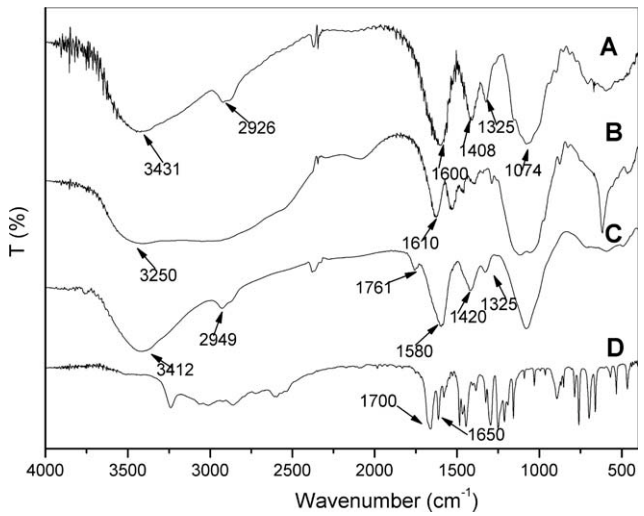

Figure 2 FTIR of (A) *O*-CMC nanoparticles, (B) gentamicin, (C) SA/GM-loaded *O*-CMC, and (D) salicylic acid.

between *O*-CMC and calcium ion, which may destroy the crystalline structure of *O*-CMC. The drugs loaded nanoparticles are amorphous, which may indicate that drugs dispersed at the molecular level in the polymer matrix and hence, no crystals were found in the drug-loaded matrices.[24,25]

In vitro release studies of GM/SA-loaded *O*-CMC nanoparticles

Drug releasing behavior of the GM/SA-loaded *O*-CMC nanoparticles was evaluated by performing the *in vitro* releasing tests in the PBS (pH 7.4). Figures 4 and 5 show the release profiles of the SA and GM from *O*-CMC nanoparticles with the different drug feeding ratio of SA to GM from 1.0 to 2.5. A burst drug release was registered in the first 1 h, followed by controlled release. The larger the feed ratio of SA to GM was, the faster the release rate of SA was. It was attributed to more amount of SA containing in formulation at the high feed ratio of SA to GM. Accordingly, the release rate of GM decreased with the increasing of feeding ratio.

Based on previous report,[26] sufficient SA (the release amount ratio of SA to GM equal or higher than 1.0 : 1.2) was required to inhibit the ototoxicity of GM. So, the release amount ratios of SA to GM depending on the different feed ratios were also investigated. The ratio between the released amounts of SA to GM was always higher than 1.0 : 1.2 in the

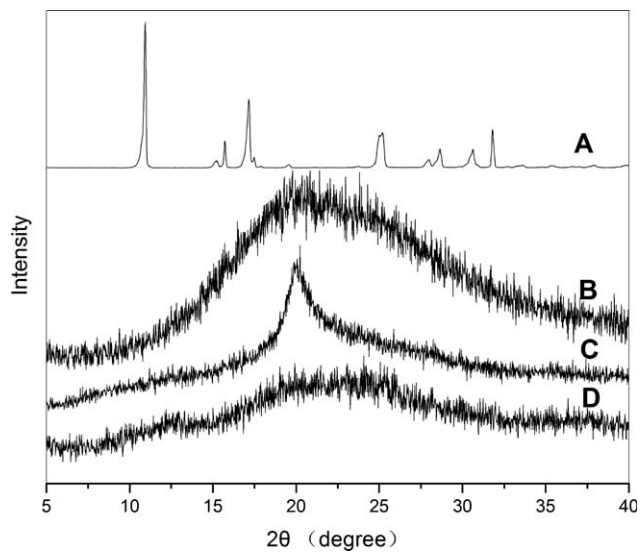

Figure 3 XRD patterns of (A) SA, (B) GM, (C) *O*-CMC, and (D) SA/GM-loaded *O*-CMC nanoparticles.

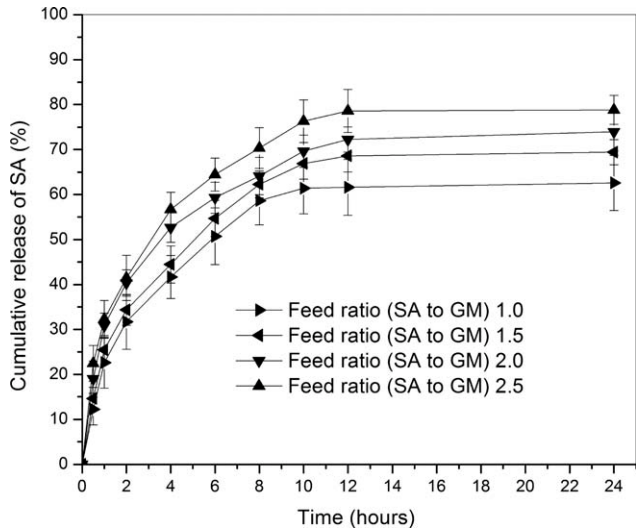

Figure 4 *In vitro* release of SA from SA/GM-loaded *O*-CMC nanoparticles with different feed ratio of SA to GM ($n = 3$).

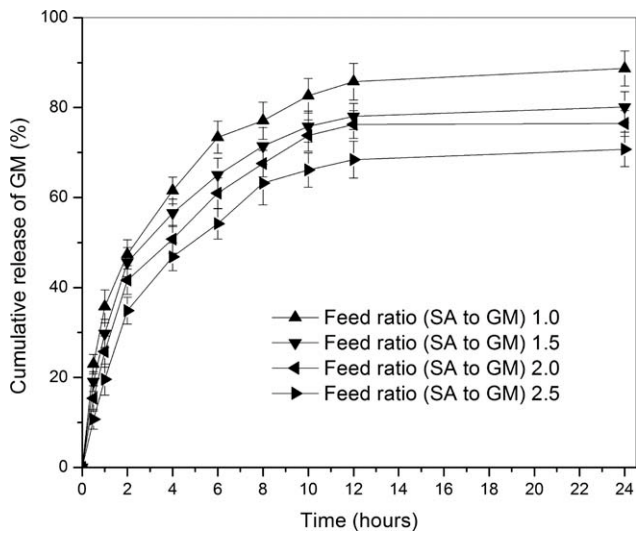

Figure 5 *In vitro* release of GM from SA/GM-loaded *O*-CMC nanoparticles with different feed ratio of SA to GM ($n = 3$).

TABLE IV
Release Kinetics of SA and GM Released from *O*-CMC Nanoparticles (mean ± SD, $n = 3$)

Feed ratio (SA to GM)	SA			GM		
	r^2	k	n	r^2	k	n
1.0	0.999	0.399 ± 0.057	0.198 ± 0.031	0.998	0.354 ± 0.039	0.224 ± 0.014
1.5	0.988	0.393 ± 0.037	0.239 ± 0.019	0.997	0.357 ± 0.033	0.204 ± 0.029
2.0	0.986	0.361 ± 0.044	0.248 ± 0.026	0.996	0.406 ± 0.042	0.208 ± 0.031
2.5	0.976	0.308 ± 0.051	0.247 ± 0.018	0.999	0.407 ± 0.038	0.174 ± 0.028

time lapse considered (24 h), except for feeding ratios of 1.0.

The release kinetic was characterized by fitting the data obtained into Korsmeyer–Peppas model. The Korsmeyer–Peppas equation was used to determine the mechanism of drug release regulating the initial portion of the time-release diagrams (i.e., $M_t/M_\infty \leq 60\%$), by using the following equation:[24]

$$\frac{M_t}{M_\infty} = kt^n$$

where M_t/M_∞ is the fraction of drug released at time t, k is the kinetic constant, and n is the diffusion exponent. In particular, $n = 0.5$ indicates that the drugs diffused and released from the polymer matrix following Fickian diffusion, while non-Fickian and anomalous diffusion kinetics are to be considered in the case of $n > 0.5$ and $n = 1$, respectively. In the Korsmeyer–Peppas model, the values of k, the correlation coefficient (r^2) and n have been calculated. The results obtained are shown in Table IV. As the feed ratio increased, the kinetic constant (k) of GM decreased and the kinetic constant (k) of SA increased. The n values of SA and GM were less than 0.5, which indicated that the drugs release was governed by non-Fickian or anomalous diffusion.[27]

CONCLUSIONS

In previous study, SA has already administered in GM-related ototoxicity treatments in the form of tablets and injection. To effectively inhibit the ototoxicity of GM by SA, *O*-CMC nanoparticles loaded with SA and GM were prepared as therapeutical agents for inhibiting the GM's ototoxicity. The preparation method was simple, mild, and did not involve the use of any acidic solvent. The prepared nanoparticles displayed spherical shape, narrow distribution, and relatively high zeta potentials. The drug release evaluated *in vitro* followed non-Fickian or anomalous diffusion kinetics, and the release amount ratio of SA to GM suggested that the *O*-CMC nanoparticles may hold great potential in antagonizing GM's ototoxicity.

References

1. Chu, J.; Niu, W. Z.; Zhang, S. L.; Zhuang, Y. P.; Hu, H.; Li, Y. R. Process Biochem 2004, 39, 1145.
2. Priuska, E. M.; Schacht, J. Biochem Pharmacol 1995, 50, 1749.
3. Sha, S. H.; Schacht, J. Hear Res 1999, 128, 112.
4. Sha, S. H.; Schacht, J. Hear Res 2000, 142, 34.
5. Song, B. B.; Sha, S. H.; Schacht, J. Free Radical Biol Med 1998, 25, 189.
6. Severinsen, S. A.; Kirkegaard, M.; Nyengaard, J. R. Hear Res 2006, 212, 99.
7. Polat, A.; Parlakpinar, H.; Tasdemir, S.; Colakc, C.; Vardi, N.; Ucar, M.; Emrea, M. H.; Acet, A. Acta Histochem 2006, 108, 365.
8. Chen, Y.; Huang, W. G.; Zha, D. J.; Qiu, J. H.; Wang, J. L.; Sha, S. H.; Schacht, J. Hear Res 2007, 226, 178.
9. Choung, Y. H.; Taura, A.; Pak, K.; Choi, S. J.; Masuda, M.; Ryan, A. F. Neuroscience 2009, 161, 214.
10. Agnihotri, S. A.; Mallikarjuna, N. N.; Aminabhavi, T. M. J Controlled Release 2004, 100, 5.
11. Kumari, A.; Yadav, S. K.; Yadav, S. C. Colloids Surf B 2010, 75, 1.
12. Soppimath, K. S.; Aminabhavi, T. M.; Kulkarni, A. R.; Rudzinski, W. E. J Controlled Release 2001, 70, 1.
13. Sayın, B.; Somavarapu, S.; Li, X. W.; Sesardic, D.; Senel, S.; Alpar, O. H. Eur J Pharm Sci 2009, 38, 362.
14. Wan, A. J.; Sun, Y.; Li, H. L. J Appl Polym Sci 2009, 114, 2639.
15. Zhang, Y. F.; Yin, P.; Zhao, X. Q.; Wang, J.; Wang, J.; Ren, L.; Zhang, Q. Q. Mater Sci Eng C 2009, 29, 2045.
16. Sun, Y.; Wan, A. J. J Appl Polym Sci 2007, 105, 552.
17. Liu, Z. H.; Jiao, Y. P.; Zhang, Z. Y. J Appl Polym Sci 2007, 103, 3164.
18. Sun, L. P.; Du, Y. M.; Fan, L. H.; Chen, X.; Yang, J. H. Polymer 2006, 47, 1796.
19. Anitha, A.; Rani, V. V. D.; Krishna, R.; Sreeja, V.; Selvamurugan, N.; Nair, S. V.; Tamurab, H.; Jayakumar, R. Carbohydr Polym 2009, 78, 672.
20. Wang, S. L.; Jiang, T. Y.; Ma, M. X.; Hua, Y. C.; Zhang, J. H. Int J Pharm 2010, 386, 249.
21. Prabaharan, M.; Reis, R. L.; Mano, J. F. React Funct Polym 2007, 67, 43.
22. Sun, S. L.; Wang, A. Q. J Hazard Mater 2006, 131, 103.
23. Wan, A.; Sun, Y.; Gao, L.; Li, H. L. Carbohydr Polym 2009, 75, 566.
24. Rokhade, A. P.; Agnihotri, S. A.; Patil, S. A.; Mallikarjuna, N. N.; Kulkarni, P. V.; Aminabhavi, T. M. Carbohydr Polym 2006, 65, 243.
25. Rokhade, A, P.; Patil, S. A.; Aminabhavi, T. M. Carbohydr Polym 2007, 67, 605.
26. Song, B. B.; Schacht, J. Hear Res 1996, 94, 87.
27. Mundargi, R. C.; Shelke, N. B.; Rokhade, A. P.; Patil, S. A.; Aminabhavi, T. M. Carbohydr Polym 2008, 71, 42.